

COMPETENCE KINETIC AND THERMODYNAMIC STUDIES BETWEEN NATURAL BIO-ADSORBENT GREEN MICROALGAE AND SYNTHETIC ADSORBENT MAGNETIC NANOPARTICLES FOR COPPER(II) ION IN WATER

Shireen Ibrahim Hamadamin¹, Sewgil Saaduldeen Anwer^{1,2*}, Kwestan Hassan Sidiq³ and Parween Mohsin Abdulkareem^{4*}

¹Hawler Medical University, College of Health Sciences, Clinical Biochemistry Department, Iraq

²Tishk International University, Nursing Faculty, Nursing Department, Iraq

³Hawler Medical University, College of Health Sciences, Medical Microbiology Department, Iraq

⁴Department of Biology, Faculty of Science and Health, Koya University, Koya KOY45, Kurdistan Region, Iraq

(Received June 13, 2022; Revised August 16, 2022; Accepted August 18, 2022)

ABSTRACT. The present work investigated the kinetic and thermodynamic study of adsorbents to remove copper ions from aqueous solutions and compared the efficiency between the natural microalgae bio-adsorbent *chlorella* species (sp.) and synthetic magnetic nanoparticles. All materials synthesized and characterized by Fourier transform infrared (FT-IR), scanning electron microscope (SEM), energy dispersive X-ray (EDX). The highest Cu⁺² ion adsorption for the copper solution at 100 mg/L was 57.2%, while at pH 8 it was 59.7%. The more efficient adsorbent for Cu⁺² acquired by *chlorella* was 0.24 mg/g. The second-order kinetic model is fitted, the activation energy (E_a) for the three adsorbents; *Chlorella*, Fe₃O₄, (Fe₃O₄ coated with SiO₂) were 95.24, 40.69, 20.39 kJ/mol, respectively indicating the adsorption process is slower than the magnetic nanoparticles. Enthalpy activation changes (ΔH^o) were endothermic and showed that the adsorption of the Cu⁺² on the *chlorella* was chemisorption and on the magnetic nanoparticles was physisorption. Entropy change of activation (ΔS^o), and activation Gibbs free energy change (ΔG^o) showed that adsorption process of Cu⁺² on the three adsorbents was feasible and spontaneous in temperature range 293-313 K. The novelty of this work is to determine the type and efficiency of adsorption of algae and nanoparticles.

KEY WORDS: Adsorption, Kinetic models, Thermodynamic studies, *Chlorella* species, Magnetic nanoparticle, Efficiency percent

INTRODUCTION

Copper ion is the essential trace element in leaving organism; for preserving healthy metabolism, the optimum Cu⁺² ion concentration is about 1.4–2.1 mg/kg of human body mass, and the World Health Organization pointed out the lowest possible amount of copper ion should be 2 mg/L in drinking water, overtaking leads to toxic effects diarrhea, vomiting, nausea and stomach cramps, while bulk concentration effects are damaging brain, liver, kidney and other tissues. Copper(II) ion concentration arises in polluted water due to chemical leaching from the coating and pipe, or bras tap corrosion; the utilization of biogenic nanoparticle production can help to lessen environmental pollution and human health risks associated with existing manufacturing techniques [1, 2].

Organisms have proceeded to survive in settings with high metal concentrations. Algae are thought to collect heavy metals, which might be exploited to produce metallic nanoparticles naturally. Among various microorganisms, microalgae are primitive microscopic plants, and they have significant advantages as cell factories for the production of nanoparticles compared to larger plants. Algae are aquatic filamentous photosynthetic organisms that fall under the kingdom of plants. All these algae are broadly classified into two types: microalgae and macroalgae [3, 4].

*Corresponding author. E-mail: parween.mohsin@koyauniversity.org, sewgil.anwar@hmu.edu.krd
This work is licensed under the Creative Commons Attribution 4.0 International License

Traditionally, algal systems have been used as a tertiary wastewater treatment method to remove heavy metals, dyes, and other contaminants.

Magnetic nanoparticles (MNPs) are biocompatible have unusual magnetic characteristics, high electrical resistivity, and chemical stability that led to much attraction. The activity of Fe_3O_4 MNPs is known to be highly dependent on their size, shape, and crystal phase [5-7]. Fe_3O_4 MNPs with an inorganic silica coating SiO_2 prevents the corrosion of Fe_3O_4 MNPs and is compatible with chemicals for bioconjugation. Features of magnetic-ordering events in materials with a magnetic field decreased dimension, potentially resulting in new technology uses [8].

The present research seeks to detect the more competent adsorbent between natural green microalga (using *Chlorella* sp.) and synthetic magnetic nanoparticles by calculating their adsorption capacity and the optimum condition for removing Cu^{+2} ion concentration in drinking water.

EXPERIMENTAL

Chemicals

Iron(II) sulfate heptahydrate ($\text{FeSO}_4 \cdot 7\text{H}_2\text{O}$, Fluka, 86-90% purity), sodium nitrate (NaNO_3 , 99%), and sodium hydroxide (NaOH , 99%) were purchased from Fluka. Ammonium hydroxide solution (NH_3 , ALPHA, 99%), absolute ethanol ($\text{C}_2\text{H}_5\text{OH}$, GCC, 99.9%), tetraethyl orthosilicate (TEOS, $\text{C}_8\text{H}_{20}\text{O}_4\text{Si}$, Merck, $\geq 99\%$), acetic acid glacial (CH_3COOH , Scharlau, 99.8%), acetylacetone ($\text{C}_5\text{H}_8\text{O}_2$, Riedel-deHaën, 99.5%), and tetra isopropyl orthotitanate (TIPO, $\text{C}_{12}\text{H}_{28}\text{O}_4\text{Ti}$, Merck, $\geq 98\%$) were used. All chemicals are analytical grade are used without extra purification.

Instrumentation

Hot plate and magnetic stirrer (Shin Saeug co., Ltd, SHPM-10, TJ19-SHPM-11), oven (memmert GmbH, U30, 801337), ultrasonic water bath (Powersonic 405, Hawshin technology Co. Korea). Aqualytic AL800 Portable Spectrophotometer, Germany. FT-IR spectroscopy Mod IR Affinity-1 CE, Shimadzu, Japan using KBr disc. Scanning electron microscopy (SEM) and energy dispersive X-ray (EDX) analyzed by Nova Nanosem 230 [FEI. USA], X-Ray diffraction (XRD) type SRN-120M [SOONA, Korea] SRN-120 [SORONA, Korea]. Shaking water bath and light microscope were also used. The analytical techniques were used for the identification, and structural analysis, chemical and physical characterization of the samples are investigated in Kurd central research facility, Soran District, Erbil City, Iraq.

Preparation of bio-adsorbent Chlorella sp.

Samples of microalgae were collected in the Greater Zab River, Iraq during May-September 2021. Water samples from the depth (10-50) cm were taken and plated on blue-green 11 medium (BG11) Merck KGaA, Darmstadt, Germany in Microbiology Laboratory, College of Health Sciences; purified on BG11 and observed under a light microscope to verify the purity of *Chlorella* sp. The cultures in each flask were centrifuged for 20 min at 5000 rpm, dried at 50 °C in an oven, and ground as described by Abdulkareem and Anwer [9].

Preparation of synthetic adsorbent core-shell ($\text{Fe}_3\text{O}_4/\text{SiO}_2$) nanoparticles

First, for preparation of Fe_3O_4 nanoparticle, a magnetic stirrer was used for stirring and dissolving two solutions of 2.6 g (0.37 M $\text{FeSO}_4 \cdot 7\text{H}_2\text{O}$) and 1.5 g (0.7 M NaNO_3) in 25 mL of distilled water until maintained 80 °C temperature, then 10 mL (2.5 M). NaOH solution was poured into the mixture with continuous stirring at 80 °C for 30min, the product left to be cooled down in room

temperature then washed and separated several times by using an external magnetic field, dried overnight at 50 °C and the black color of the product was weighed obtaining 76% of the nanoparticle. Then the prepared ferrous(III) oxide Fe₃O₄ nanoparticle (45 mg) were ultrasonicated in 16 mL of distilled water for 60 min, then 2 mL ammonium hydroxide (24 wt%) with 80 mL ethanol was added to the first solution followed by adding 0.8 mL of tetraethyl orthosilicate (TEOS) in drops with stirring at room temperature, then stirring continued for 24 h, washing and separating the nanoparticle by external magnetic field several times with distilled water. The brown product was dried and collected at 50 °C [10].

Characterization of magnetic nanoparticles

Visual observation was used to track the color change in the combination containing the Fe₃O₄ and core-shell Fe₃O₄/SiO₂. To confirm nanoparticle formation, each of the samples was conducted by the Fourier transforms infrared (FT-IR) analysis in which powdered samples were mixed with potassium bromide and pressed as KBr pellet. The typical infrared scan was created in the mid-infrared from 4000 to 400 wave-numbers at a resolution of cm⁻¹. Furthermore, the size, morphology observation, and composition of nanoparticles identified by scanning electron microscope (SEM), energy dispersive X-ray (EDX), and X-ray diffraction (XRD) to provide information regarding the crystalline structure and grain size [11].

Copper ion adsorption experiments

Batch adsorption experiments were performed at a different initial copper ion concentration (100, 200, 300, 400, 500 mg/L), various pH solutions (6.5, 7, 7.5, 8, 8.5), and temperature (20, 25, 30, 35, 40 °C) according to Aksu [12]. After completing the agitation time for 18 h in a shaking water bath with the speed of 120 rpm then the adsorbent was filtered and the supernatant was analyzed by the solid-single-beam spectrophotometer with an excellent performance ratio that is specifically designed for water testing for the absorbance measurements at 560 nm using bicinchoninate method. The yield of removal and adsorption capacities for heavy metals was determined using the following formula:

$$\text{Removal \% of heavy metals} = (C_o - C_e/C_o) \times 100 \quad (1)$$

The adsorption capacities were determined using equation 2.

$$q_e = [(C_o - C_e)V]/W \quad (2)$$

where q_e is the amount of Cu(II) ion adsorbed per unit of adsorbents (mg/g), C_o and C_e are the initial and equilibrium concentrations of Cu(II) ion in the solution (mg/L), V is the volume of Cu(II) ion solution (L) and W is the weight of the particle adsorbents (g) [12].

Adsorption kinetics and thermodynamics

Studying adsorption kinetic is very important to comprehend the rate of the adsorption of Cu⁺² ion on the surface of the adsorbents. The kinetic models (Lagergren model), pseudo second order, and second-order models with their linear plots as shown in equation 4:

$$\frac{dA_t}{dt} = k_1(A_{eq} - A_t) \quad (3)$$

$$\ln(A_{eq} - A_t) = \ln A_{eq} - k_1 t \quad (4)$$

where A_{eq} and A_t are the absorbance of Cu⁺² ions at equilibrium time and time t, respectively, k₁ is the pseudo-first-order rate constant (1/h), and t is the time (h). The values of k₁ and A_{eq} can be

determined from the slope and intercept of the linear plot $\ln(A_{eq}-A_t)$ versus t as shown in equation (4) [13]. Pseudo-second-order rate equation

$$\frac{dA_t}{dt} = k_1(A_{eq} - A_t)^2 \quad (5)$$

$$t/A_t = 1/k_2 A_{eq}^2 + t/A_{eq} \quad (6)$$

where k_2 is the pseudo-second-order rate constant (L/mol.h) is determined from the slope and intercept (A_{eq}) of the linear plot of t/A_{eq} against t as shown in equation 6.

Second-order rate equation

$$R = k_2[Cu^{+2}][adsorbent] \quad (7)$$

$$A_t / (A_{eq}(A_{eq} - A_t)) = k_2 t \quad (8)$$

where R is the rate of reaction of the Cu^{+2} ion concentration and concentration of each adsorbents *Chlorella* species or nanoparticle. By plotting $A_t/(A_{eq}(A_{eq}-A_t))$ against t and determining k_2 (second-order rate constant (L/mol.h)) from the slope [14].

The activation energy (E_a) (kJ/mol) determined from the Arrhenius equation, which is the minimum energy for preceding the reaction as shown in equation 9

$$\ln k = \ln A - E_a/RT \quad (9)$$

where A is the Arrhenius factor, R is the gas constant (8.314 J/mol. K), and T is the absolute temperature (K). By plotting $\ln k_2$ of the second-order constant versus inverse temperature ($1/T$), a straight line is obtained with a slope of $-E_a/R$, where E_a can be determined.

The activation thermodynamic parameters, enthalpy variation (ΔH^\ddagger), the entropy variation (ΔS^\ddagger), and the Gibbs free energy variation (ΔG^\ddagger) can be obtained using equations 10, 12, and 13:

$$\Delta H^\ddagger = E_a - RT \quad (10)$$

$$A = (ek_b T/h)e^{\Delta S^\ddagger/R} \quad (11)$$

$$\Delta S^\ddagger = R(\ln A - \ln(\frac{ek_b T}{h})) \quad (12)$$

$$\Delta G^\ddagger = \Delta H^\ddagger - T\Delta S^\ddagger \quad (13)$$

where k_b is the Boltzmann constant equal to 1.3806×10^{-23} J/K and h is the Plank constant equal to 6.626×10^{-34} Js [15, 16].

RESULTS AND DISCUSSION

Characterization of the bio-adsorbent Chlorella sp.

The unicellular *Chlorella* sp. Cultured on BG11 medium and the pure culture was examined under a microscope to confirm the algal strain. The algae appeared as spherical, unicellular green colour with disc-shaped chloroplast; the morphological characteristics of the current study were similar to the Iraqi strains of *Chlorella* identified by [17, 18] they revealed that the isolated strains of microalgae from Koya city were belongs to the species *Chlorella Vulgaris*. The production of synthesise of metallic nanoparticles ferrous(III) oxide Fe_3O_4 nanoparticles appeared as black colored (Figure 1).



Figure 1. (a) *Chlorella* under light microscope, (b) *Chlorella* biomass, and (c) Fe_3O_4 nanoparticles appeared as black coloured.

Characterization of the synthetic adsorbent nanoparticles

FT-IR is a time-saving, nondestructive approach for detecting various functional groups and is sensitive to changes in molecular structure. The information provided by FT-IR is based on the chemical composition and physical condition of the entire sample. The FT-IR spectrum of metallic nanoparticles is shown in Figure 2. A strong absorption band appears around the region 600 cm^{-1} in FT-IR spectra (a) and (b) are for stretching vibration of the Fe-O bending vibration. In comparison, the bands at 1082.07 cm^{-1} in the ranges (b) indicate non-symmetrical shape without aggregation with the asymmetric stretching band for Si-O-Si. The bands between $1400\text{-}1700\text{ cm}^{-1}$ were appeared in spectra (c) and not present in spectra (a) and (b) due to cellulose functional group of *Chlorella species* like $\nu(\text{C}=\text{O})$ stretching of ester, protein amid bands $\nu(\text{C}=\text{O})$ stretching, $\delta(\text{N-H})$ bending and $\nu(\text{C-N})$ stretching.

One of the ideal tools that can resolve individual MNPs and the structure of their associated Nano trusses is scanning electron microscopy (SEM). The images of the prepared nanoparticles have been taken in different modulation, as review SEM images shown with 100kx magnification all the nanoparticles have nonsymmetrical crystalline shape, and the morphology of the magnetic nanoparticles with the surface of algae (*Chlorella*) were carried out on MIRA3 TESCAN as shown in Figure 3. The average particle size of the magnetic nanoparticles was obtained as follows 50-57 nm Fe_3O_4 , core-shell $\text{Fe}_3\text{O}_4/\text{SiO}_2$ 57-88.9 nm, and pure *Chlorella* was 130 nm.

The morphology of magnetic nanoparticles and pure *Chlorella* sp. cell surface were observed by SEM in which the nanoparticles appeared as spherical to nonsymmetric crystalline shaped nanoparticles with agglomeration, which may occur during processing with high temperature; Yufanyi and co-authors demonstrated a significant correlation between SiO_2 's photodegradation performance and its crystallite size and structural progression [19]. By using SEM pictures, Munasir and coauthors investigated the structural analysis of $\text{Fe}_3\text{O}_4/\text{SiO}_2$ and crystalline SiO_2 particles [20]. The outcome showed that the amorphous phase and the crystalline phase have distinct particle sizes and morphologies. These outcomes came from the observation made by [21].

The compositional information of each nanoparticle is elaborated by overviewing the energy dispersive X-ray technique, each EDX spectra are shown in Figure 4, where silicone element is found in ranges (b) core-shell $\text{Fe}_3\text{O}_4/\text{SiO}_2$ with the percent 5.28% indicating the shell of SiO_2 , while a percent of other features like carbon, nitrogen, sulfur, phosphorus, potassium, magnesium and aluminum are presented in spectra (h) indicating the *chlorella* functional groups.

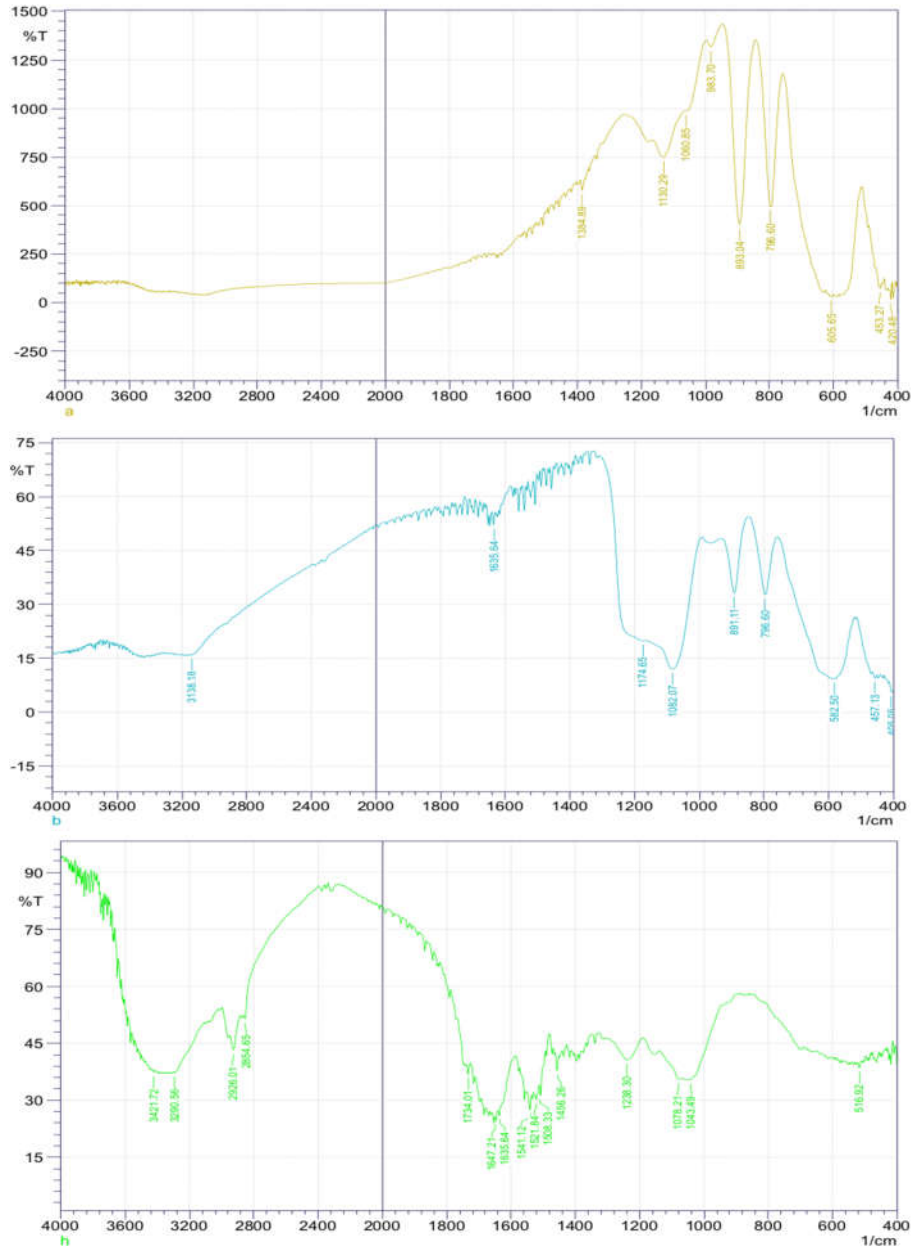


Figure 2. FT-IR spectra of (a) Fe_3O_4 , (b) core-shell $\text{Fe}_3\text{O}_4/\text{SiO}_2$, and (c) untreated *Chlorella* sp.

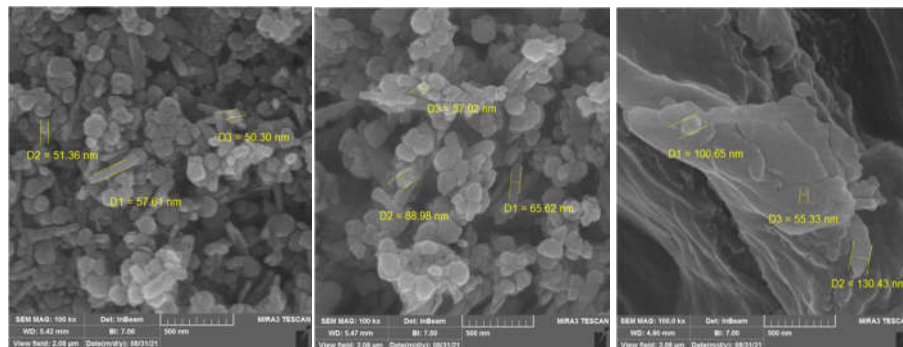


Figure 3. SEM manograph of (a) Fe₃O₄ MNPs, (b) core-shell Fe₃O₄/SiO₂ MNPs, and (h) untreated *Chlorella* sp.

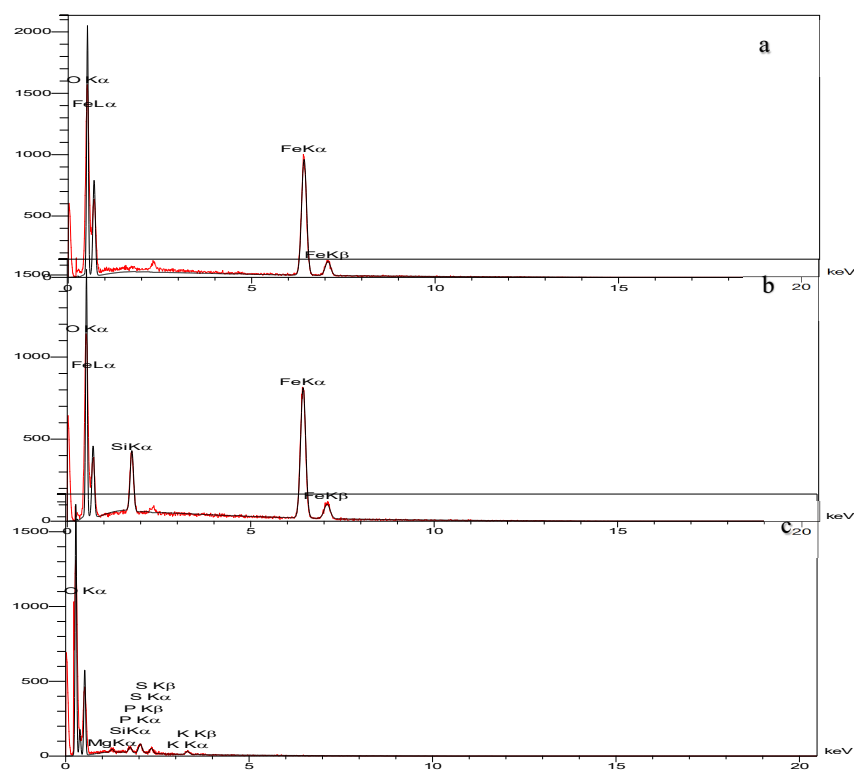


Figure 4. EDX of (a) Fe₃O₄ MNPs, (b) core-shell Fe₃O₄/SiO₂ MNPs, and (c) untreated *Chlorella*.

Effect of Cu²⁺ ion concentrations and pH on the adsorption process

The effect of the initial Cu²⁺ ion concentration in the range (100-500 mg/L) on 0.3 g *Chlorella* sp. algae and MNPs are shown in Figures 5A and B. The best removal is displayed at 12th h., and the fast removal is displayed at 3th hours. The maximum adsorption of Cu²⁺ was recorded at a low concentration of 100 mg/L (57.2 %). By increasing the metal ion concentration, the biosorption process is reduced the competitive dispersion of metal ions has risen at the sites available on the adsorbent surface at high concentrations; these pores are closed, and metal ions are prevented from going deep into the adsorbent pores, implying that adsorption occurs exclusively on the surface, Putri and colleagues concluded that decline in adsorption, indicating saturation of all the binding sites on the algal surface [22]. The maximum adsorption capacities of *Scenedesmus armatus* and *Chlorell avulgaris* against zinc, Pb²⁺, and Cd²⁺ ions were demonstrated by Zabochnicka-Witek and Ryga at the lowest sorbent concentrations [23].

pH is one of the most important parameters influencing the rate and strength of the initial adsorption. This effect is due to the chemical reaction between each heavy metal and the algal cell walls. Hydrogen ion also serves as a bridge between the microalgal cell wall and the heavy metal molecules. To find a suitable pH for the effective heavy metal biosorption by *Chlorella* sp., experiments were performed at five different initial pH values 6.5, 7, 7.5, 8, 8.5, the effect of initial pH on the heavy metal biosorption of *Chlorella* and MNPs are given in Figures (5C and D). Maximum removal of Cu²⁺ ion showed at pH 8 (59.7%) by *Chlorella*. König-Péter and co-authors [24] stated that the biosorption process was successful at pH 5–6 for Pb²⁺ and pH 4–6 for Cd²⁺ adsorption the difference in this result with the present result is due to the difference in functional groups on the cell surface of microalgae. Removal of copper ion from aqueous solution by MNPs investigated by [25] and they showed that the pH effect was discovered to have a significant role in copper elimination that magnetic nanoparticles might be useful in wastewater treatment. As the pH increases, the density of the proton decreases, and the biomass layer is more negatively charged.

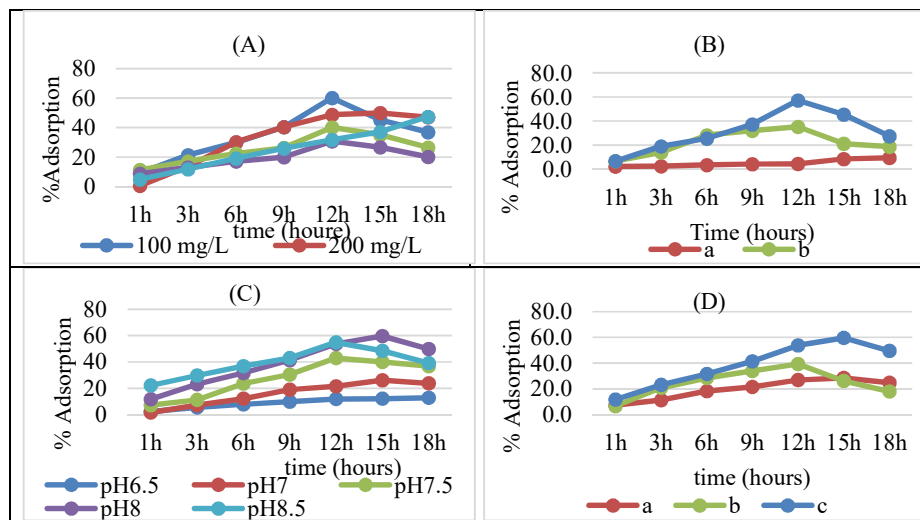


Figure 5. Effect of Cu²⁺ ion concentration on the adsorption process by (A) 0.3 g of untreated *Chlorella* sp. (B) effect of 0.3 g of each adsorbent on 100 mg/L of Cu²⁺ ion concentration (C) effect of pH on the Cu²⁺ ion adsorption by (C) Untreated *Chlorella* sp. (D) effect of pH 8 on each adsorbent a - Fe₃O₄, b - core-shell Fe₃O₄/SiO₂, c - untreated *Chlorella* species.

Effect of temperature on the adsorption process

Temperature is the critical parameter that highly affects adsorption behavior. The study was done at five different initial temperature values of 293, 298, 303, 308, and 313 K; the impact of temperature on Cu^{+2} ion adsorption on *Chlorella* sp. and MNPs are shown in Figures 6 a, b and c. the nanoparticle adsorbents are rapidly reached to equilibrium at 12 h while *chlorella* sp. at 15 h at all temperature range. The adsorption percent and capacity for each natural and synthetic adsorbent are exhibited in the Table 1.

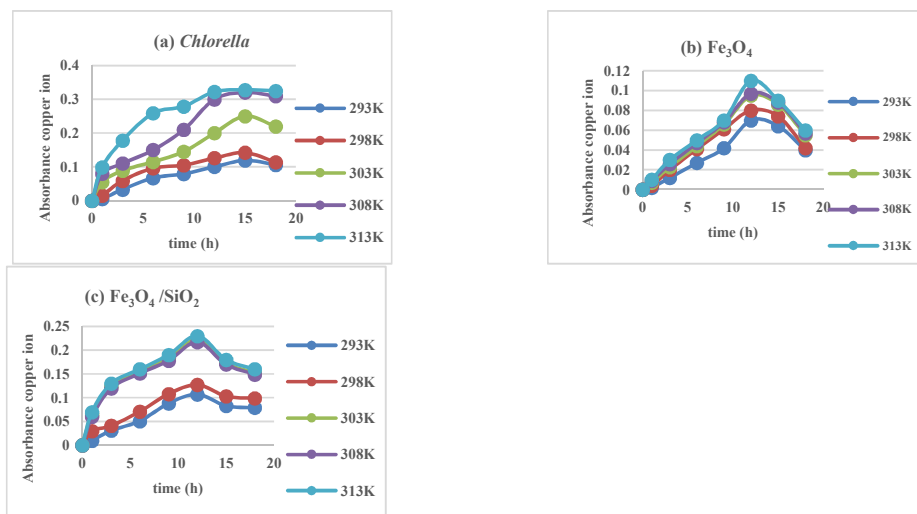


Figure 6. Kinetic adsorption copper(II) ion with time(h) in the temperature range 293-313 K for 0.3 g of each adsorbents (a) *chlorella* spices, (b) Fe_3O_4 MNPs, (c) Fe_3O_4 coated with SiO_2 MNPs.

Table 1. Adsorption capacity and adsorption efficiency of Cu^{+2} ion by natural bio-adsorbent *Chlorella* sp. and synthetic nanoparticles.

Adsorbents	C_0 (mg/L)	Time (h)	C_e (mg/L)	q_e (mg/g)	% Adsorption
<i>Chlorella</i> sp.	128	15	87.8	0.24	79.1
Core-shell $\text{Fe}_3\text{O}_4/\text{SiO}_2$ MNPs	118.8	12	63.1	0.16	53.2
Fe_3O_4 MNPs	122	12	30.4	0.06	24.9

The uptake of Cu^{+2} ions from the aqueous solution on each adsorbent *Chlorella species* and Fe_3O_4 nanoparticle and Fe_3O_4 coated with SiO_2 using three kinetic models pseudo-first-order, pseudo-second-order, and second-order models are summarized in Table 2. The second-order rate showed the highest value of correlation coefficient (R^2) range 0.97-0.99 indicating the rate of adsorption process is depending on the concentration of both Cu^{+2} ion and the adsorbents concentration.

Comparing the value of the rate constant k_2 between two adsorbent, increased gradually with increasing temperature, the synthetic adsorbent k_2 values are higher than the natural adsorbent, the range (1.27-2.54)L/mol.h, (0.57-1.6)L/mol.h, and (0.13-1.76)L/mol.h are for the adsorbents

Fe₃O₄ coated with SiO₂ nanoparticle, Fe₃O₄ nanoparticle, and *Chlorella* spices, respectively. This can be attributed to the increase in collisions probability between the active sites SiO₂ chelating the copper ions more and decreases in the boundary layer thickness as compared to the *Chlorella* spices and finally increasing the rate of adsorption [26].

Table 2. Kinetic models and variables for the adsorption of copper(II) ion with temperature on 0.3 g of each adsorbents *chlorella* spices, Fe₃O₄, and Fe₃O₄ coated with SiO₂ nanoparticles.

Kinetic models		Lagergren pseudo-first-order			Pseudo-second-order			Second order	
linear equation		$\ln(A_{eq}-A_t) = \ln A_{eq} - k_1 t$			$t/A_t = 1/k_2 A_{eq}^2 + t/A_{eq}$			$A_t/(A_{eq}(A_{eq}-A_t)) = k_2 t$	
Adsorbent	Temp (K)	A _{eq}	k ₁ (1/h)	R ²	A _{eq}	k ₂ (L/mol.h)	R ²	k ₂ (L/mol. h)	R ²
Chlorella	293	0.123	0.129	0.98	0.268	0.182	0.84	0.139	0.98
	298	0.139	0.1593	0.97	0.191	0.788	0.97	0.22	0.98
	303	0.226	0.0087	0.95	0.337	0.253	0.78	0.61	0.99
	308	0.296	0.1059	0.96	0.73	0.068	0.57	0.71	0.97
	313	0.293	0.213	0.97	0.427	0.558	0.98	1.76	0.98
Fe ₃ O ₄	293	0.074	0.102	0.97	0.123	0.239	0.93	0.575	0.98
	298	0.088	0.158	0.96	0.275	0.104	0.50	0.843	0.96
	303	0.1	0.129	0.97	0.093	1.185	0.72	1.422	0.98
	308	0.101	0.131	0.98	0.278	0.126	0.61	1.533	0.98
	313	0.111	0.11	0.99	0.245	0.188	0.56	1.608	0.99
Fe ₃ O ₄ /SiO ₂	293	0.12	0.18	0.91	0.983	0.100	0.47	1.279	0.99
	298	0.134	0.19	0.92	0.177	0.755	0.67	1.599	0.98
	303	0.196	0.18	0.97	0.233	1.587	0.99	1.785	0.99
	308	0.193	0.18	0.98	0.232	1.480	0.99	1.801	0.99
	313	0.201	0.183	0.97	0.238	1.658	0.99	2.544	0.99

From the Arrhenius plot of the $\ln k_2$ against $1/T(K)$ obtaining activation energy E_a from the slope and $\ln A$ from the intercept for each adsorbent (a) *chlorella* spices, (b) Fe₃O₄ nanoparticle, (c) Fe₃O₄ coated with SiO₂ nanoparticles are shown in the Figures (7a, b, and c) and all the thermodynamic values are summarized in the Table 3. The magnitude of the activation energy for each adsorbent *chlorella*, Fe₃O₄ MNP, and Fe₃O₄ coated with SiO₂ MNP are 92.24, 40.69, and 20.39 kJ/mol, respectively, indicating the adsorption of copper ion on the natural adsorbent *chlorella* species are slower than the synthetic adsorbents MNPs.

The thermodynamic activation parameters were illustrated in the table (3) for the adsorption of copper ion on the adsorbent enthalpy change ΔH^\ddagger are positive value indicating the adsorption is endothermic in nature; also the type of adsorption process can be determined from the value of enthalpy value, the adsorption of Cu²⁺ ion on the natural bio adsorbent *Chlorella spices* ΔH^\ddagger was high 92 kJ/mol (higher than 40 kJ/mol) which is a chemisorption type, the force was similar to a chemical bond while Cu adsorption on synthetic magnetic nanoparticles were physisorption type where ΔH^\ddagger values 38 and 17 kJ/mol for Fe₃O₄ MNPs and Fe₃O₄ coated with SiO₂ MNPs respectively (lower than 40 kJ/mol), the Cu²⁺ was held at the surface MNP adsorbents by Vander Waals force [27].

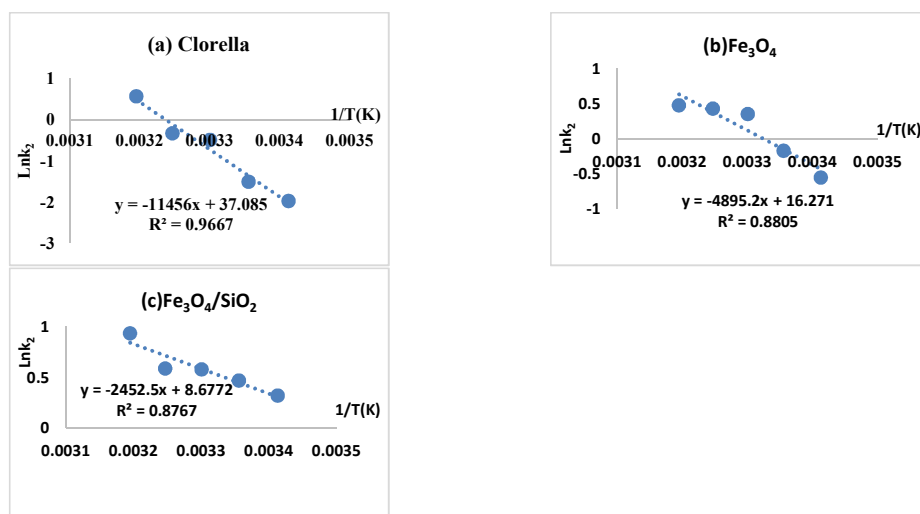


Figure 7. Arrhenius plot for each adsorbent (a) *chlorella* spices, (b) Fe_3O_4 MNPs, and (c) Fe_3O_4 coated with SiO_2 MNPs.

Table 3. Thermodynamic activation parameters for the adsorption of copper (II) ions on 0.3 g of each adsorbent's *chlorella* spices, Fe_3O_4 MNPs, and Fe_3O_4 coated with SiO_2 MNPs.

Adsorbents	Temp (K)	k_2 (L/mol. h)	1/T(k)	$\text{Ln}k_2$	$E^\#$ (kJ/mol)	A-factor (L/mol. h)	$\Delta H^\#$ (kJ/mol)	$\Delta S^\#$ (kJ/mol.K)	$\Delta G^\#$ (kJ/mol)
<i>Chlorella</i>	293	0.140	0.0034	-1.967	95.2450	1.2×10^{16}	92.809	1.365	-307.230
	298	0.222	0.0034	-1.505			92.768	1.365	-314.057
	303	0.614	0.0033	-0.489			92.726	1.365	-320.882
	308	0.719	0.0032	-0.329			92.684	1.365	-327.707
	313	1.767	0.0032	0.569			92.643	1.365	-334.531
Fe_3O_4 MNPs	293	0.576	0.0034	-0.552	40.6980	91.1×10^7	38.263	1.192	-311.074
	298	0.844	0.0034	-0.170			38.221	1.192	-317.035
	303	1.422	0.0033	0.352			38.180	1.192	-322.995
	308	1.533	0.0032	0.427			38.138	1.192	-328.955
	313	1.608	0.0032	0.475			38.096	1.192	-334.914
$\text{Fe}_3\text{O}_4/\text{SiO}_2$ MNPs	293	1.380	0.0034	0.322	20.3900	5867.6	17.954	1.129	-312.884
	298	1.600	0.0034	0.470			17.913	1.129	-318.529
	303	1.785	0.0033	0.579			17.871	1.129	-324.174
	308	1.801	0.0032	0.588			17.829	1.129	-329.818
	313	2.544	0.0032	0.934			17.788	1.129	-335.461

CONCLUSION

Copper(II) ion adsorption on bio-adsorbent *Chlorella* spices and synthetic adsorbent MNPs are strongly affected by initial ion concentration, pH, and temperature. The main and vastly utilized copper ion adsorbent concluded in this research was natural bio-adsorbent green algae (*Chlorella* sp.) are slower than synthetic magnetic nanoparticles. The Cu^{+2} ion adsorption process on the *chlorella* spices is chemical adsorption, while on the synthetic MNPs are, physical adsorption, and both types of the adsorbent obtained are spontaneous, endothermic, and Normal adsorption processes.

ACKNOWLEDGMENT

The Ministry of Higher Education supported the study, Hawler Medical University, College of Health Sciences, Kurdistan Region, Iraq.

REFERENCES

1. Ala, A.; Walker, A.P.; Ashkan, K.; Dooley, J.S.; Schilsky, M.L. Wilson's Disease. *Lancet* **2007**, *369*, 397-408.
2. Tchounwou, P.B.; Yedjou, C.G.; Patlolla, A.K.; Sutton, D.J. Heavy metal toxicity and the environment. *Exp. Suppl.* **2012**, *101*, 133-64.
3. Leaf, M.C.; Gay, J.S.A.; Newbould, M.J.; Hewitt, O.R.; Rogers, S.L. Calcareous algae and cyanobacteria. *Geol. Today* **2020**, *36*, 75-80.
4. Taghizadeh, S.M.; Berenjian, A.; Chew, K.W.; Show, P.L.; Mohd Zaid, H.F.; Ramezani, H.; Ghasemi, Y.; Racee, M.J.; Ebrahimezhad, A. Impact of magnetic immobilization on the cell physiology of green unicellular algae *Chlorella vulgaris*. *Bioengineered* **2020**, *11*, 141-153.
5. Kim, K.S. Functionalization of magnetic nanoparticles for biomedical applications. *Korean J. Chem. Eng.* **2014**, *31*, 1289-1305.
6. Huang, Q.; Zou, L.; Chen, D. Phase and morphology controlled in the synthesis of iron oxide particles: Dimension-based carbonaceous materials as modifiers. *RSC Adv.* **2016**, *6*, 82294-82297.
7. Fatima, H.; Lee, D.W.; Yun, H.J.; Kim, K.S. Shape-controlled synthesis of magnetic Fe₃O₄ nanoparticles with different iron precursors and capping agents. *RSC Adv.* **2018**, *8*, 22917-22923.
8. Chen, Y.; Chen, Q.; Mao, H.; Lin, Y.; Li, J. Preparation of magnetic nanoparticles via a chemically induced transition: presence/absence of magnetic transition on the treatment solution used. *J. Chem.* **2016**, 7604748.
9. Abdulkareem, P.M.; Anwer, S. Biosorption of cadmium and lead using microalgae spirulina sp. isolated from Koya City (Iraq). *Appl. Ecol. Environ. Res.* **2020**, *18*, 2657-2668.
10. Han, J.; Seok, G. A preparation of dual-layered core-shell Fe₃O₄-SiO₂ nanoparticles and their properties of plasmid DNA purification. *Nanomaterials* **2021**, *11*, 3422.
11. Slater, T.; Janssen, A.; Camargo, P.; Burke, M.; Zaluzec, N.; Haig, S. STEM-EDX tomography of bimetallic nanoparticles: A methodological investigation. *Ultramicroscopy* **2016**, *162*, 61-73.
12. Aksu, Z. Application of biosorption for the removal of organic pollutants: a review. *Process Biochemistry* **2005**, *40*, 997-1026.
13. Mohamed, N.A.; Al-Harby, N.F.; Almarshed, M.S. Enhancement of adsorption of Congo Red dye onto novel antimicrobial trimellitic anhydride isothiocyanate-cross-linked chitosan hydrogels. *Polym. Bull.* **2020**, *77*, 6135-6160.
14. Ho, Y.S. Second-order kinetic model for the sorption of cadmium onto tree fern: A comparison of linear and non-linear methods. *Water Res.* **2006**, *40*, 119-125.
15. Atkins, P.W.; Paula J.D. *Atkins Physical Chemistry*, 8th ed., Oxford: New York; **2006**; p. 809.
16. Skoog, D.A.; Holler, F.J.; Crouch, S.R. *Principles of Instrumental Analysis*, 6th ed., Thomson: Canada; **2007**; p. 501.
17. Allen, M.M. Simple conditions for growth of unicellular blue-green algae on plantes. *J. Phycol.* **1968**, *4*, 1-13.
18. Abdulkareem, P.M. *Induced wastewater treatment and biodiesel production using microalgae isolated from Koya distinct*. PhD Thesis, Koya University, Koya, Iraq, **2020**.

19. Yufanyi, D.; Ondoh, A.; Foba-Tendo, J.; Mbadcam, K. J. Effect of decomposition temperature on the crystallinity of α -Fe₂O₃ (hematite) obtained from an iron(III)-hexamethylenetetramine precursor. *Am. J. Chem.* **2015**, *5*, 1-9.
20. Munasir; Dewanto, A.S.; Kusumawati, D.H.; Putri, N.P.; Yulianingsih, A.; Sa'adah, I.K.F.; Taufiq, A.; Hidayat, N.; Sunaryono, S.; Supardi, Z.A.I. Structure analysis of Fe₃O₄@SiO₂ core shells prepared from amorphous and crystalline SiO₂ particles. *IOP Conference Series: Mater. Sci. Eng.* **2018**, *367*, 012010.
21. Salem D.; Ismail M.; Aly-Eldeen M. Biogenic synthesis and antimicrobial potency of iron oxide (Fe₃O₄) nanoparticles using algae harvested from the Mediterranean Sea, Egypt. *Egypt. J. Aquatic Res.* **2019**, *45*, 197-204.
22. Putri, L.S.E.; Dewi, P.S.; Dasumiati. Adsorption of Cd and Pb using biomass of microalgae *Spirulina platensis*. *Int. J. Geomater.* **2017**, *13*, 121-126.
23. Zabochnicka-Świątek, M.; Rygała, A. The effect of biomass (*Chlorella vulgaris*, *Scenedesmus armatus*) concentrations on Zn²⁺, Pb²⁺ and Cd²⁺ biosorption from zinc smelting wastewater. *Inżynieria i Ochrona Środowiska* **2017**, *20*.
24. König-Péter, A.; Kilár, F.; Felinger, A.; Pernyeszi, T. Biosorption characteristics of *Spirulina* and *Chlorella* cells for the accumulation of heavy metals. *J. Serb. Chem. Soc.* **2015**, *80*, 407-419.
25. Al-Jabri, M.; Devi M.; Al-Abri M. Synthesis, characterization and application of magnetic nanoparticles in the removal of copper from aqueous solution. *Appl. Water Sci.* **2018**, *8*, 223.
26. El-Harby, N.F.; Ibrahim, S.M.A.; Mohamed, N.A. Adsorption of Congo Red dye onto antimicrobial terephthaloyl thiourea cross-linked chitosan hydrogels. *Water Sci. Technol.* **2017**, *76*, 2719-2732.
27. Zhu, N.; Yan, T.; Qiao, J.; Cao, H. Adsorption of arsenic, phosphorus and chromium by bismuth impregnated biochar: Adsorption mechanism and depleted adsorbent utilization. *Chemosphere* **2016**, *164*, 32-40.